Differential evolution based adaptation for the direct current motor velocity control parameters

Miguel G. Villarreal-Cervantes[a,*], Efrén Mezura-Montes[b], José Yaír Guzmán-Gaspar[c]

[a]*Mechatronic section, Posgraduate Department, Instituto Politécnico Nacional, CIDETEC, Mexico, D.F., 07700, Mexico*
[b]*Artificial Intelligence Research Center, University of Veracruz, Sebastián Camacho 5, Centro, Xalapa, Veracruz, 91000, Mexico*
[c]*National Laboratory of Advanced Informatics (LANIA A.C.), Rébsamen 80, Centro, Xalapa, Veracruz, 91000, Mexico*

Abstract

The adaptively design of the control system for a direct current motor is solved by proposing differential evolution based control adaptation (DEBAC). From the comparison of two differential evolution variants with two constraint-handling techniques, a competitive algorithm based on arithmetic crossover and a set of feasibility rules is obtained. In addition, a comparison of such competitive differential evolution variant against a traditional control technique considering stabilization and tracking is provided. Based on the empirical results, the proposed approach outperforms the traditional method by using three well-known performance indices for closed-loop control, confirming that DEBAC is a valid alternative to control the direct current motor under parametric uncertainties.

Keywords:
Bio-inspired adaptive control, differential evolution, bio-inspired optimization, DC motor, velocity control.

*Corresponding author: E-mail address: mvillarrealc@ipn.mx

List of acronyms

The paper adopts the following acronyms:

EAs	Evolutionary algorithms
CTEAs	Control tuning using EAs
d.o.f.	Degree of freedom
DOP	Dynamic optimization problem
DE	Differential evolution
DC	Direct Current
PID controller	Proportional Integral and Derivative controller
DEBAC	Differential evolution based adaptive control
CHM	Constraint-handling method
iRace package	Iterated Racing for Automatic Algorithm Configuration package
TVP	Time-variant parameters
$TVP1$	Time-variant parameters that change its nominal value by 10% in the time interval $t \in [2, 4]s$
$TVP2$	Time-variant parameters that change its nominal value by 10% in the time interval $t \in [0, 4]s$
EP	Exterior penalization
DF	Deb's feasibility
DEC2B-EP	DE/Current-to-best/ with EP
DEB1B-EP	DE/Best/1/bin/ with EP
DEC2B-DF	DE/Current-to-best/ with DF
DEB1B-DF	DE/Best/1/bin/ with DF
RCP	Regulation control problem
TCP	Tracking control problem
RCP-TVP1	Regulation control problem with TVP1 parameter
RCP-TVP2	Regulation control problem with TVP2 parameter
TCP-TVP1	Tracking control problem with TVP1 parameter
TCP-TVP2	Tracking control problem with TVP2 parameter
NomP	Nominal parameters
PIC	Proportional-Integral control
IAE	Integral Absolute Error
ITAE	Integral Time-weighted Absolute Error
ISE	Integral Squared Error
S.D.	Standard Deviation

1. Introduction

A high performance control system in the actuators of an electro-mechanical system is a crucial factor to be considered in several applications. The Direct Current (DC) motor is the most used actuator for electromechanical systems, such as robot manipulator [27], in xy table [28], etc. The study of control strategies in the DC motor with a high precision and high accuracy has always been of interest [15, 19].

One important issue in the tuning of control systems is to compensate the uncertain parameters in electromechanical systems when those are used in tasks, such as,

handling different loads in the robot end-effector, polishing rough surfaces or when the system physical parameters are affected by temperature changes, system mass variation (vehicles), wide operating range, etc.

Although advanced control system theory [2, 26, 11, 21] and tuning strategies were developed to improve the controller performance, in the last years evolutionary algorithms (EAs) [8], whose inspiration is taken from the natural evolution theory and the survival of the fittest, have been used as another alternative for controller tuning [9, 23]. One of the EA advantages is that they do not require gradient information and work as black-box optimizers (i.e., they are independent of the features of the problem to be solved). EAs have showed a very competitive performance when solving complex optimization problems [25], as those related with the automatic control area, mainly because their global search capabilities and their ability to deal with non-linearity and discontinuous problems. In addition, they are easier to implement than advanced control tuning. EAs were designed to deal with unconstrained search spaces, then a constraint-handling technique must be added to it so as to consider feasibility information in the search bias [16]. However, the choice of the correct constraint-handler is an open problem [16] in the control tuning using EAs (CTEAs). Several researches in CTEAs have been used different ways of handling constraints. In [24], a differential evolution (DE) variant *DE-curent-to-rand/2* is considered to obtain the proportional gain, the integral time, the derivative time and the parameter of the derivative filter to the Proportional-Integral-Derivative (PID) control system for a first order system with delay. One performance function related to the disturbance rejection is chosen and three constraints are set (the robustness of the closed-loop system, the maximum limits of the control signal and the sensitivity under noise signals). In order to handle the constraints, the performance function evaluation changes to the sum of the constraint violation if the obtained solution is

unfeasible. In [1] a multi-objective genetic algorithm (MOGA) is used to select the optimum control gains for the desired drug dose, considering both, the number of proliferating cells at the end of the cancer chemotherapy treatment and the average level of toxicity over the whole period of treatment, as performance functions. The stability of the closed-loop system, maximum toxicity and drug concentration at tumor site are set as constraints in the optimization process. Those constraints are included into the performance function as penalty functions in order to handle such constraints in the MOGA. Another approach to handle the constraints in the CTEAs is to consider them as performance functions [10] where a multi-objective optimization problem is stated.

Some other works include EAs and other nature-inspired algorithms in the adaptive control schemes. In [13] an adaptive particle swarm optimization (APSO) algorithm is proposed to adaptively select the optimum the elements of state weighting matrix Q and the input weighting matrix R of linear quadratic regulator (LQR) control for the tracking of a two degrees of freedom (d.o.f.) laboratory helicopter. Adaptive inertia weight factor (AIWF) is introduced in the velocity update equation of PSO and a feed forward controller linearizes the closed-loop system in order to solve an unconstrained optimization problem with the proposal. The APSO algorithm significantly improves the control performance compared with the conventional PSO. In [29] the adaptation of the rule base parameters, member function parameters and scaling factors of a fuzzy controller are obtained by stated an unconstrained optimization problem and by using a real-number coding genetic algorithm. This approach is applied to a permanent magnet synchronous motor. The comparison between the performance of the bacterial foraging algorithm and genetic algorithm is carried out in [4] for the identification and control of a DC motor. The results indicate that both algorithms have a similar performance in the error velocity but

the main difference is the time consuming for the dynamic performance.

From the literature review, it is clear that EAs are a valid option to deal with complex problems of the automatic control area to efficiently tune the control system. On the other hand, they are initial applications in this particular area of one of the most recent EAs known as differential evolution (DE), whose usage to solve complex optimization problems has significantly increased due to its good performance and simplicity [6]. However, to the best of the authors' knowledge, there is a lack of information about the performance behavior of the constraint-handling into the EAs for the optimal control tuning with parametric uncertainties. The research on the type of DE variant which is more suitable to deal with those constrained search spaces of automatic control instances and also investigations about the most convenient constraint-handling technique are still scarce. Therefore, the main contribution of this research is two-fold: *i*) The proposal of an alternative approach called DEBAC to control the velocity of the DC motor under parametric uncertainties based on an evolutionary adaptive control, and *ii*) the empirical analysis of the most representative DE variants for faster convergence coupled with two competitive constraint-handling techniques is carried out in order to get information about their performance on the velocity control of the DC motor under parametric uncertainties.

From the above mentioned, a DE-based adaptive control (DEBAC) for a DC motor is proposed by the formal statement of a dynamic optimization problem (DOP) and its solution is given by comparing the performance of two DE variants based on arithmetic crossover and discrete crossover, with two different constraint-handling technique. The proposed DEBAC on-line estimates the control parameters to compensate the non-linear effect of parametric uncertainties in the velocity control of a DC motor. Furthermore, a comparison of the most competitive DE variant against a traditional control technique is also presented.

The rest of the paper is organized as follows: In Section 2, the DC motor dynamic model is presented. The dynamic optimization problem for the on-line control parameter estimation is stated in Section 3. A brief introduction to DE is included in Section 4. In Section 5, the comparative analysis of those DE variants in the particular DOP and the comparison against a traditional control technique are discussed. Finally, in Section 6 conclusions are given and the future work is proposed.

2. Dynamic model and velocity control system of the DC motor

The electromechanical equations related to the DC motor are given in (1) and (2) and those can be derived by using the Kirchhoff's voltage law and Newton's 2nd law, respectively. The equation (1) is the electrical circuit equation of armature and the equation (2) is the mechanical equation of DC motor, for more details consult [5], [12].

$$L_a \frac{di_a}{dt} + R_a i_a + k_e \dot{q}_m = V_{in} \tag{1}$$

$$J_o \frac{d\dot{q}_m}{dt} + b_o \dot{q}_m + \tau_L = k_m i_a \tag{2}$$

Both previous equations are named as the dynamic model of the DC motor where V_{in} is the armature voltage, R_a is the armature resistance, L_a is the armature inductance, k_e is the back electromotive constant, i_a is the armature current, b_0 is the viscous friction coefficient of the motor shaft bearing, J_0 is the inertia torque of the motor rotor, k_m is the torque constant, τ_L is the load torque and q_m, $\dot{q}_m$, $\ddot{q}_m$ are the position, velocity and acceleration of the rotor, respectively.

Let the state variable vector $x = [q_m, \dot{q}_m, i_a]^T$ and the input signal $u = V_{in}$, and considers the parameters of the DC motor as $p = [p_1 = \frac{b_0}{J_0}, p_2 = \frac{k_m}{J_0}, p_3 = \frac{k_e}{L_a}, p_4 =$

$\frac{R_a}{L_a}, p_5 = \frac{1}{L_a}, p_6 = \frac{\tau_L}{J_0}]^T$ then, the dynamic model of the DC motor in the state variable vector x can be expressed in state-variable form $\dot{x} = f\left(x(t), u(t), p\right)$ as in (3).

$$\begin{bmatrix} \dot{x}_1 \\ \dot{x}_2 \\ \dot{x}_3 \end{bmatrix} = \begin{bmatrix} 0 & 1 & 0 \\ 0 & -p_1 & p_2 \\ 0 & -p_3 & -p_4 \end{bmatrix} \begin{bmatrix} x_1 \\ x_2 \\ x_3 \end{bmatrix} - \begin{bmatrix} 0 \\ p_6 \\ 0 \end{bmatrix} + \begin{bmatrix} 0 \\ 0 \\ p_5 \end{bmatrix} u \tag{3}$$

Considering the coordinate change $\tilde{x}_1 = x_2$, $\tilde{x}_2 = -p_1 x_2 + p_2 x_3 - p_6$, the dynamic system (3) can be expressed as in (4)-(5), where $\tilde{x}_3 = \frac{\tilde{x}_2 + p_6 + p_1 \tilde{x}_1}{p_2}$.

$$\dot{\tilde{x}}_1 = \tilde{x}_2 \tag{4}$$

$$\dot{\tilde{x}}_2 = p_2 p_5 u + \tilde{x}_1(p_2 p_3 - p_1^2) + \tilde{x}_3 p_2(p_1 + p_4) \tag{5}$$

From (4)-(5), the inverse dynamic control $u(t) = \tilde{f}(x(t), \bar{p})$ is proposed to regulate the velocity of the DC motor and it is given in (6), where $e = w_r - x_2(t)$ is the error between the desired angular velocity w_r, and the current angular velocity $x_2(t)$, $\dot{e} = \dot{w}_r - \dot{x}_2(t)$ is the error between the desired angular acceleration $\dot{w}_r$ and the current angular acceleration $\dot{x}_2(t)$, $\ddot{w}_r$ is the rate of change of the desired angular acceleration and k_p, k_d are the control gains.

$$u = \frac{\ddot{w}_r + k_p e + k_d \dot{e} + \bar{p}_1 \bar{p}_2 x_3 - \bar{p}_1^2 x_2 + \bar{p}_1 \bar{p}_6}{\bar{p}_2 \bar{p}_5} + \frac{\bar{p}_3 x_2}{\bar{p}_5} + \frac{\bar{p}_4 x_3}{\bar{p}_5} \tag{6}$$

The vector $\bar{p}$ will be the design variable vector in the control system (6). It is considered that the current parameter vector $p(t)$ in the dynamic model of the DC motor (3) dynamically changes its value affecting the dynamic behavior of the DC motor. Hence, the design variable vector in the control system must be estimated

at each sampling time Δt (online control parameter estimation) in order to compensate the non-linearity effects in the DC motor due to the variations of the current parameter vector p. In this paper the design variable vector in the control system $\bar{p}(t)$ is obtained by proposing and solving a dynamic optimization problem (DOP). Differential evolution variants are used to solve the DOP.

3. Dynamic optimization problem for the online control parameter estimation

Considering that the current parameter vector $p(t) = [p_1(t), p_2(t), p_3(t), p_4(t), p_5(t), p_6(t)]^T$ in the dynamic model of the DC motor is not constant and its value varies according to the changes in the current time variable $t \in [0, \Delta t, 2\Delta t, ..., t_f]$. Then, the dynamic optimization problem consists in finding the control design variable vector $\bar{p}(t)$ for the control system (6) that compensates the non-linear behavior of the DC motor in order to track the desired velocity, subject to the motor dynamics, the estimated dynamics of the DC motor and bounds in the input control signal. The term t_f is the final time and Δt is the sampling time. In the next subsections the performance function and constraints are presented.

3.1. Performance function

Let the time space Ω as $\Omega = \{\lambda \in R \mid \lambda \in [t_1,\ t_n] \subseteq t,\ t_1 = t_n - \Delta w, \Delta w > \Delta t,\ t_n \geq \Delta w,\ t_n > t_1\}$ and the estimated dynamics of the DC motor as $\dot{\bar{x}} = \bar{f}\left(\bar{x}(t), u(t), \bar{p}\right)$. The performance function (7) is considered as the squared difference between the estimated state vector of the estimated DC motor $\bar{x}$ and the state vector of the simulated DC motor x when $t \in \Omega$. The current time must fulfill $t \geq t_n$ in order to evaluate the performance function. The back time interval is represented as $\Delta w \in R$.

$$J = \int_{t\in\Omega} (x_1(t) - \bar{x}_1(t))^2 dt + \int_{t\in\Omega} (x_2(t) - \bar{x}_2(t))^2 dt + \int_{t\in\Omega} (x_3(t) - \bar{x}_3(t))^2 dt \quad (7)$$

3.2. Constraints

The dynamic constraints involve both the dynamic model of the DC motor (8) and the estimated one. Those dynamic constraints consist of differential equations that describe the dynamic behavior of the DC motor, such as mechanical-electrical energy balances that ensure the physical relations.

The estimated dynamics of the DC motor has the same form presented in (3) with the difference that the vector p is changed by $\bar{p}$ and the current state vector x is changed by the estimated state vector $\bar{x}$. The estimated dynamics of the DC motor is included to know the dynamic behavior of the DC motor with different design variable vector $\bar{p}(t)$ and so, to compensate the effects provided by the parameter p. In order to solve the differential equations in (8) and in (9), the Euler method is used to obtain the state vector x and $\bar{x}$, respectively. An integration step of Δt is selected in both cases. The initial condition $x(0) = [0, 0, 0]^T$ for the dynamic equation (8) is set with a final time t_f. Furthermore, the state vector $\bar{x}(t_1) = x(t_1)$ is chosen as the initial condition for the dynamic equation (9) with a final time t_n.

$$\dot{x}(t) = f(x(t), u(t), p) \quad (8)$$

$$\dot{\bar{x}}(t) = f(\bar{x}(t), u(t), \bar{p})\Big|_{t\in\Omega} \quad (9)$$

The control system presents physical limits due to the power system, hence the inequality constraints in the control signal presented in (10)-(11) are included in order to bound the applied voltage in the DC motor.

$$g_1 : u(t_n) - u_{MAX} \leq 0 \tag{10}$$

$$g_2 : u_{MIN} - u(t_n) \leq 0 \tag{11}$$

The last inequality constraint involves the design variable vector bounds and those are given in (12)-(13), where $\bar{p}_{MIN}$ and $\bar{p}_{MAX}$ are the lower and upper limits in the design variable vector $\bar{p}$.

$$g_3 : \bar{p} - \bar{p}_{MAX} \leq 0 \tag{12}$$

$$g_4 : \bar{p}_{MIN} - \bar{p} \leq 0 \tag{13}$$

3.3. Dynamic optimization problem statement

In Fig. 1 the complete process for obtaining the control parameter vector $\bar{p}$ is shown. The closed-loop system is marked in dashed line. The optimization process requires the knowledge of the state vector $x(t)$ in the time interval $t \in [t_1, t_n]$. At each time $t = t_n$, the performance function is evaluated. The required information is obtained from the state vector $x(t) \in \Omega$ and from the differential equation solution of the estimated state vector $\bar{x} \in \Omega$ considering the initial condition as $x(t_1)$.

The dynamic optimization problem consists in finding the optimum control design variable vector $\bar{p}^* = [\bar{p_1}^*, \bar{p_2}^*, \bar{p_3}^*, \bar{p_4}^*, \bar{p_5}^*, \bar{p_6}^*]^T$ that minimizes (7), i.e., the error between the state vector x and the estimated state vector $\bar{x}$ such that $\bar{p}^*$ compensate the non-linear effects on the parameter vector p of the DC motor, subject to the DC motor dynamics (8), the estimated DC motor dynamics (9), bounds in the control signal (10)-(11) and bounds in the design variable vector (12)-(13). Hence, the general formulation of the dynamic optimization problem is stated as in (14)-(20).

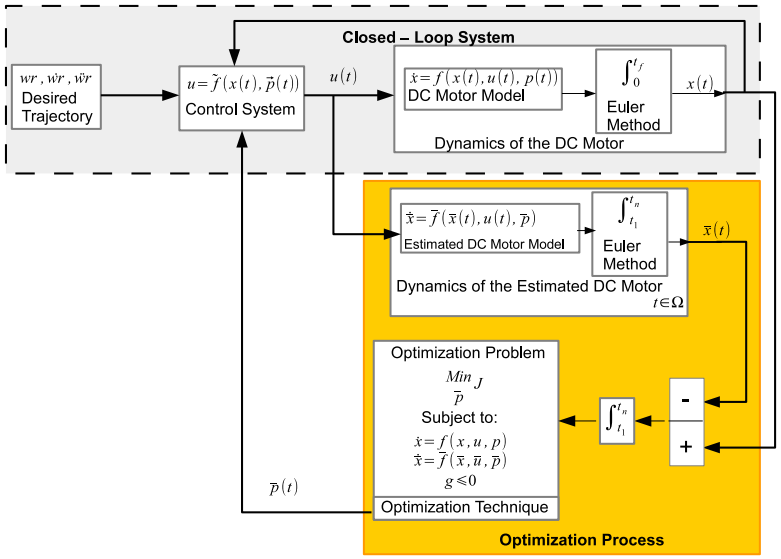

Figure 1: Schematic diagram of the dynamic optimization process for the on-line control parameter estimation.

$$\underset{\bar{p}^*}{Min} J \tag{14}$$

Subject to:

$$\frac{dx}{dt} = f(x(t), u(t), p), \qquad x(0) = [0, 0, 0]^T \tag{15}$$

$$\frac{d\bar{x}}{dt} = f(\bar{x}(t), u(t), \bar{p})\Big|_{t\in\Omega}, \quad \bar{x}(t_1) = x(t_1) \tag{16}$$

$$g_1(x(t_n), \bar{p}) \leq 0 \tag{17}$$

$$g_2(x(t_n), \bar{p}) \leq 0 \tag{18}$$

$$g_3(\bar{p}) \leq 0 \tag{19}$$

$$g_4(\bar{p}) \leq 0 \tag{20}$$

4. Differential evolution

Differential evolution [22] is an EA proposed by Storn and Price to solve optimization problem with floating-point parameters [22]. A population of NP potential solutions (where each potential solution is a control design variable vector $p(t) = [p_1(t), p_2(t), p_3(t), p_4(t), p_5(t), p_6(t)]^T$) called just vectors is generated at random with uniform distribution. Each D-dimensional vector i in the population at generation G, $\vec{x_{i,G}} = [x_{i,1,G}, x_{i,2,G}, ..., x_{i,D,G}]^T$, known as target vector, is combined with a mutant vector $\vec{v_{i,G}} = [v_{i,1,G}, v_{i,2,G}, ..., v_{i,D,G}]^T$ to generate a trial (child) vector $\vec{u_{i,G}} = [u_{i,1,G}, u_{i,2,G}, ..., u_{i,D,G}]^T$. The mutant vector $\vec{v_{i,G}}$ is generated by the so-called differential mutation, which requires three vectors $\vec{x_{r0,G}}$, $\vec{x_{r1,G}}$, and $\vec{x_{r2,G}}$, $r0 \neq r1 \neq r2 \neq i$, chosen at random from the current population. Such process is detailed in Equation (21):

$$\vec{v}_{i,G} = \vec{x}_{r0,G} + F(\vec{x}_{r1,G} - \vec{x}_{r2,G}) \tag{21}$$

where $F > 0$ is a scale factor for the difference vectors $\vec{x}_{r1,G}$ and $\vec{x}_{r2,G}$. Such difference determines a search direction which is added to the base vector $\vec{x}_{r0,G}$. After that, the crossover operator is applied to the target vector $\vec{x_{i,G}}$ and the mutant vector $\vec{v_{i,G}}$ as indicated in Equation (22)

$$u_{i,j,G} = \begin{cases} v_{i,j,G} & \text{if}(rand_j \leq CR) \text{ or } (j = J_{rand}) \\ x_{i,j,G} & \text{otherwise} \end{cases} \tag{22}$$

where $0 \leq CR \leq 1$ is the crossover parameter which determines how similar the trial vector $\vec{u_{i,G}}$ will be with respect to the mutant vector $\vec{v_{i,G}}$. $J_{rand} \in [1, D]$ is a random integer number which assures the trial vector to get at least one value copied from the mutant vector to prevent target vector copies.

As a final step, the target and trial vectors are compared based on fitness, and the best of them will remain in the population for the next generation, as shown in Equation (23), where minimization is assumed. The complete DE pseudocode is presented in Algorithm 1.

$$\vec{x}_{i,G+1} = \begin{cases} \vec{u}_{i,G} & \text{if}(f(\vec{u}_{i,G}) \leq f(\vec{x}_{i,G})), \\ \vec{x}_{i,G} & \text{otherwise} \end{cases} \tag{23}$$

The DE variant already described is known as DE/rand/1/bin, where *"DE"* stands for differential evolution, *"rand"* indicates the criterion to choose the base vector $\vec{x}_{r0,G}$ (at random), *"1"* means the number of differences (one based on two vectors) and *"bin"* refers to the type of crossover operator (binomial in this case as shown in Equation (22)). However, there are other variants like DE/best/1/bin, where the only difference is that the base vector is the best solution in the current population $\vec{x}_{best,G}$. The corresponding mutant vector calculation is detailed in Equation (24). After that, the binomial crossover in Equation (22) is applied in the same way as in DE/rand/1/bin.

$$\vec{v}_{i,G} = \vec{x}_{best,G} + F(\vec{x}_{r1,G} - \vec{x}_{r2,G}) \tag{24}$$

There are other DE variants, also based on the best vector in the population as the base vector, like DE/current-to-best/1, where an arithmetic crossover is used instead of a discrete recombination like binomial crossover. The formula for this variant is detailed in Equation (25).

$$\vec{u}_{i,G} = \vec{x}_{i,G} + K(\vec{x}_{best,G} - \vec{x}_{i,G}) + F(\vec{x}_{r1,G} - \vec{x}_{r2,G}) \tag{25}$$

It is important to note that the trial vector $\vec{u}_{i,G}$ is directly generated in Equation

Algorithm 1 Differential Evolution algorithm

G=0
Create a randomly-generated initial population $\vec{x}_{i,G}\,\forall i, i = 1, \ldots, NP$
Evaluate $f(\vec{x}_{i,G})\,\forall i, i = 1, \ldots, NP$
for $G \leftarrow 1$ to MAX_GEN **do**
  for $i \leftarrow 1$ to NP **do**
    Randomly select $r0 \neq r1 \neq r2 \neq i$
    $J_{rand} = randint[1, D]$
    for $j \leftarrow 1$ to D **do**
      if $rand_j \leq Cr$ Or $j = J_{rand}$ **then**
        $u_{i,j,G} = x_{r0,j,G} + F(x_{r1,j,G} - x_{r2,j,G})$
      else
        $u_{i,j,G} = x_{i,j,G}$
      end if
    end for
    if $f(\vec{u}_{i,G}) \leq f(\vec{x}_{i,G})$ **then**
      $\vec{x}_{i,G+1} = \vec{u}_{i,G}$
    else
      $\vec{x}_{i,G+1} = \vec{x}_{i,G}$
    end if
  end for
end for

(25) (i.e., no mutant vector $\vec{v}_{i,G}$ is considered in this case). Therefore, the binomial crossover is not adopted for DE/current-to-best/1 because the recombination and mutation are carried out in the same Equation (25).

Specialized literature suggests that those DE variants whose base vector is the best solution in the population provide a faster convergence than those where the base vector is chosen at random [18, 17]. Based on such behavior and also on the fact that the DE variants in this research will operate on-line, DE/best/1/bin and DE/current-to-best/1 are the variants of interest. Details of an in-depth analysis on other DE variants in constrained search spaces can be found in [17].

Recalling from Section 1, DE, as all EAs, were not designed to deal with constrained search spaces. A recent review of the state-of-the-art in nature-inspired constrained optimization, showed that DE is one of the most popular EAs adopted to solve constrained optimization problems [16]. Furthermore, two of the most competitive constraint-handling techniques nowadays are the exterior penalty functions [3] and the set of feasibility rules [16]. Therefore, they are adopted in this study.

The penalized fitness function $\bar{J}$ of a vector $(\vec{x}_{i,G})$ is given in Equation (26), where μ is the penalty factor, and n_g is the number of constraints g.

$$\bar{J}(\vec{x}_{i,G}) = J(\vec{x}_{i,G}) + \sum_{i=1}^{n_g} \mu(max(0, g_i(\vec{x}_{i,G})))^2 \tag{26}$$

The set of feasibility rules proposed by Deb [7] are three criteria adopted to select solutions based on feasibility and they are the following:

- ◇ Any feasible solution is preferred to any infeasible solution.
- ◇ Between two feasible solutions, the one having better objective function value is preferred.
- ◇ Between two infeasible solutions, the one having smaller sum of constraint violation $SCV = \sum_{i=1}^{n_g}(max(0, g_i(\vec{x}_{i,G})))^2$ is preferred.

The pseudocodes of DE/best/1/bin and DE/current-to-best/1, where each one of

the two constraint-handling techniques (penalty function or Deb's feasibility rules) can be used, are presented in Algorithms 2 and 3, respectively.

5. Results

The simulation tests were designed to asses the performance of two DE variants described in Section 4, both using the two constraint-handling techniques already introduced. Therefore, four DE variants were considered: $Best/1/bin/EP$, $Best/1/bin/DF$, $Curret-to-best/EP$ and $Current-to-best/DF$, where the last term refers to the constraint-handling technique: EP means exterior penalty-function, while DF stands for Deb's feasibility-rules. After the four DE variants comparison, the most competitive is further compared against a traditional automatic control technique.

The algorithms were coded in Matlab on a 64-bit Windows operating systems, with Intel Core $i5-3317U$ processor (1.70 GHz) and $4GB$ of RAM. The parameter values of the DE variants were obtained by using the Iterated Racing for Automatic Algorithm Configuration (iRace) package [14], a parameter tuning tool which finds the most suitable settings for an EA. The obtained parameters and the short name for each DE variant are presented in Table 1. All runs stop after 900 evaluations of the performance function for the parameter tuning process and for the simulation tests reported in this document. Additionally, the upper limits of the design variable vector $\bar{p}$ were chosen as in Table 2 and those were selected according to a decrease of at most 25% in the nominal parameters of the DC motor showed in Table 3. The lower limits are set to zero because the DC motor parameter variations can not be negative. Only $\bar{p}_{MAX_6}$ includes both positive and negative bound values due to the consideration of positive or negative load torque uncertainties applied to the motor shaft. In addition, it is considered bounds of the applied voltage as $u_{MAX} = 70V$,

Algorithm 2 DE/best/1/bin

G=0
Create a randomly-generated initial population $\vec{x}_{i,G}\,\forall i, i = 1, \ldots, NP$
Evaluate $J(\vec{x}_{i,G})$, each constraint $g_j(\vec{x}_{i,G})\,\forall j, j = 1, \ldots, n_g$ and the SCV $\forall i, i = 1, \ldots, NP$
if Penalty function is used **then**
  Calculate $\bar{J}(\vec{x}_{i,G})$ based in Equation 26
end if
for $G \leftarrow 1$ to MAX_GEN **do**
  for $i \leftarrow 1$ to NP **do**
    Randomly select $r1 \neq r2 \neq i$
    $J_{rand} = randint[1, D]$
    for $j \leftarrow 1$ to D **do**
      if $rand_j \leq Cr$ Or $j = J_{rand}$ **then**
        $u_{i,j,G} = x_{best,j,G} + F(x_{r1,j,G} - x_{r2,j,G})$
      else
        $u_{i,j,G} = x_{i,j,G}$
      end if
    end for
    if Penalty function is used **then**
      if $\bar{J}(\vec{u}_{i,G}) \leq \bar{J}(\vec{x}_{i,G})$ **then**
        $\vec{x}_{i,G+1} = \vec{u}_{i,G}$
      else
        $\vec{x}_{i,G+1} = \vec{x}_{i,G}$
      end if
    else
      if $SCV(\vec{u}_{i,G}) = 0$ And $SCV(\vec{x}_{i,G}) > 0$ **then**
        $\vec{x}_{i,G+1} = \vec{u}_{i,G}$
      else if $SCV(\vec{u}_{i,G}) > 0$ And $SCV(\vec{x}_{i,G}) = 0$ **then**
        $\vec{x}_{i,G+1} = \vec{x}_{i,G}$
      else if $SCV(\vec{u}_{i,G}) = 0$ And $SCV(\vec{x}_{i,G}) = 0$ **then**
        if $J(\vec{u}_{i,G}) < J(\vec{x}_{i,G})$ **then**
          $\vec{x}_{i,G+1} = \vec{u}_{i,G}$
        else
          $\vec{x}_{i,G+1} = \vec{x}_{i,G}$
        end if
      else
        if $SCV(\vec{u}_{i,G}) < SCV(\vec{x}_{i,G})$ **then**
          $\vec{x}_{i,G+1} = \vec{u}_{i,G}$
        else
          $\vec{x}_{i,G+1} = \vec{x}_{i,G}$
        end if
      end if
    end if
  end for
end for

Algorithm 3 DE/current-to-best/1

G=0
Create a randomly-generated initial population $\vec{x}_{i,G}\,\forall i, i = 1, \ldots, NP$
Evaluate $J(\vec{x}_{i,G})$, each constraint $g_j(\vec{x}_{i,G})\,\forall j, j = 1, \ldots, n_g$ and the SCV $\forall i, i = 1, \ldots, NP$
if Penalty function is used **then**
  Calculate $\bar{J}(\vec{x}_{i,G})$ based in Equation 26
end if
for $G \leftarrow 1$ to MAX_GEN **do**
  for $i \leftarrow 1$ to NP **do**
    Randomly select $r1 \neq r2 \neq i$
    $J_{rand} = randint[1, D]$
    for $j \leftarrow 1$ to D **do**
      $\vec{u}_{i,G} = \vec{x}_{i,G} + K(\vec{x}_{best,G} - \vec{x}_{i,G}) + F(\vec{x}_{r1,G} - \vec{x}_{r2,G})$
    end for
    if Penalty function is used **then**
      if $\bar{J}(\vec{u}_{i,G}) \leq \bar{J}(\vec{x}_{i,G})$ **then**
        $\vec{x}_{i,G+1} = \vec{u}_{i,G}$
      else
        $\vec{x}_{i,G+1} = \vec{x}_{i,G}$
      end if
    else
      if $SCV(\vec{u}_{i,G}) = 0$ And $SCV(\vec{x}_{i,G}) > 0$ **then**
        $\vec{x}_{i,G+1} = \vec{u}_{i,G}$
      else if $SCV(\vec{u}_{i,G}) > 0$ And $SCV(\vec{x}_{i,G}) = 0$ **then**
        $\vec{x}_{i,G+1} = \vec{x}_{i,G}$
      else if $SCV(\vec{u}_{i,G}) = 0$ And $SCV(\vec{x}_{i,G}) = 0$ **then**
        if $J(\vec{u}_{i,G}) < J(\vec{x}_{i,G})$ **then**
          $\vec{x}_{i,G+1} = \vec{u}_{i,G}$
        else
          $\vec{x}_{i,G+1} = \vec{x}_{i,G}$
        end if
      else
        if $SCV(\vec{u}_{i,G}) < SCV(\vec{x}_{i,G})$ **then**
          $\vec{x}_{i,G+1} = \vec{u}_{i,G}$
        else
          $\vec{x}_{i,G+1} = \vec{x}_{i,G}$
        end if
      end if
    end if
  end for
end for

$u_{MIN} = -70V$ and this must be set according with the maximum/minimum nominal voltage of the DC motor. The penalty factor was set to $\mu = 1000$ through a trial and error procedure in order to greatly penalize the performance function when unfeasible individuals are given

In the simulation tests, both, the regulation and the tracking control problems [26] were taken into consideration. The references for the regulation control problem and for the tracking control problem were $w_r = 40rad/s$ and $w_r = 40\sin(6.28t)rad/s$, respectively. In both cases, the gains of the inverse dynamic control (6) were set as $k_p = 34524$, $k_d = 368$ through a rigours trial and error procedure where the used values in the paper are those that provide the best performance function among trials. The simulation parameters of the closed loop system considered an integration step of $\Delta t = 5ms$ and a final time of $t_f = 6s$. The selection of the control gains were given by a rigours trial and error procedure where such values are those that provide the best performance function among trials. In order to provide uncertainties in the nominal parameters of the DC motor, represented in Table 3, time-variant parameters of the DC motor were incorporated in the simulation tests. Two different time-variant parameters were regarded for both control problems: Parameter $TVP1$: Time-variant parameters can only change its nominal value by 10% in the time interval $t \in [2, 4]s$ and they are expressed in Table 4. Parameter $TVP2$: Time-variant

Table 1: Parameters of the DE variants by using the iRace package.

DE variant	Nomenclature	K	CR	F	NP	Δw
$DE/Current-to-best/EP$	DEC2B-EP	0.6302	-	0.3567	42	10
$DE/Current-to-best/DF$	DEC2B-DF	0.8684	-	0.4281	112	9
$DE/Best/1/bin/EP$	DEB1B-EP	-	0.8118	0.4019	50	10
$DE/Best/1/bin/DF$	DEB1B-DF	-	0.8869	0.5639	65	9

Table 2: Limits of the design variable vector $\bar{p}$.

	$\bar{p}_{MAX_1}$	$\bar{p}_{MAX_2}$	$\bar{p}_{MAX_3}$	$\bar{p}_{MAX_4}$	$\bar{p}_{MAX_5}$	$\bar{p}_{MAX_6}$
$\bar{p}_{MAX}$	2	1200	5	100	10	150
$\bar{p}_{MIN}$	0	0	0	0	0	-150

Table 3: Nominal parameters (NomP) of the DC Motor.

NomP	**Value**	**Unit**
J_0	0.000345	Nms^2
k_m	0.394600	Nm
b_0	0.000585	Nms^2
R_a	9.665000	Ω
k_e	0.413300	$V/rads$
L_a	0.102440	H
τ_L	0	Nm

parameters can change its nominal value by 10% all time interval, i.e., $t \in [0, t_f = 6]s$ and they are expressed in Table 5. For closed loop simulation results, time-variant parameters were included as $p = \breve{p}$. It is important to point out that the time-variant parameters of the DC motor have different frequencies in order to highly perturb the dynamics of the motor.

5.1. Performance analysis of the DE variants

Ten independent runs were carried by each DE variant (**DEC2B-EP**, **DEC2B-DF**, **DEB1B-EP**, **DEB1B-DF**) for each control problem than involves two different DC motor parameters (TVP1 and TVP2) i.e., the control problems were: regulation control problem with TVP1 parameter (RCP-TVP1), regulation control

Table 4: Parameter TVP1: Time-variant parameters (TVP) of the DC motor. Those can be grouped in $\breve{p} \in R^6$.

TVP	**Value** $\forall$ **t** $\in [\mathbf{2}, \mathbf{4}]$	**Value** $\forall$ **t** $\notin [\mathbf{2}, \mathbf{4}]$	**Unit**
$\breve{J}_0$	$J_0 + 0.10 J_0 sin(2.0943t)$	J_0	Nms^2
$\breve{k}_m$	$k_m + 0.10 k_m sin(6.2831t)$	k_m	Nm
$\breve{b}_0$	$b_0 + 0.10 b_0 sin(3.1415t)$	b_0	Nms^2
$\breve{R}_a$	$R_a + 0.10 R_a sin(2.0943t)$	R_a	Ω
$\breve{k}_e$	$k_e + 0.10 k_e sin(6.2831t)$	k_e	$V/rads$
$\breve{L}_a$	$L_a + 0.10 L_a sin(3.1415t)$	L_a	H
$\breve{\tau}_L$	0	τ_L	Nm

problem with TVP2 parameter (RCP-TVP2), tracking control problem with TVP1 parameter (TCP-TVP1), tracking control problem with TVP2 parameter (TCP-TVP2).

In Table 6 the error velocity norm $\|\dot{e}(t)\| \ \forall \ t \in [1.6, 6]s$ is given by each DE variant per single run. The error velocity norm is computed from the settling time of $1.6s$. Only the results with acceptable behavior are showed i.e., the results with trajectory velocity error less than 5% with respect to the desired velocity trajectory. Otherwise, a dash is included for unacceptable results. The number of unacceptable results for each DE variant were: four with the DEB1B-EP (in *RCP-TVP2*), two with the DEB1B-DF (in *RCP-TVP1* and *RCP-TVP2*), two with the DEC2B-EP (in *RCP-TVP1* and *RCP-TVP2*) and one using DEC2B-DF (in *RCP-TVP2*). Such results indicate that all DE variants are reliable for the tracking control problem (TCP) but in the regulation control problem (RCP) the more reliable DE variant was DEC2B-DF which only presented one unacceptable result. When using the

Table 5: Parameter TVP2: Time-variant parameters (TVP) of the DC motor. Those can be grouped in $\breve{p} \in R^6$.

TVP	**Value** $\forall$ $\mathbf{t} \in [\mathbf{0}, \mathbf{t_f}]$	**Unit**
$\breve{J}_0$	$J_0 + 0.10 J_0 sin(2.0943t)$	Nms^2
$\breve{k}_m$	$k_m + 0.10 k_m sin(6.2831t)$	Nm
$\breve{b}_0$	$b_0 + 0.10 b_0 sin(3.1415t)$	Nms^2
$\breve{R}_a$	$R_a + 0.10 R_a sin(2.0943t)$	Ω
$\breve{k}_e$	$k_e + 0.10 k_e sin(6.2831t)$	$V/rads$
$\breve{L}_a$	$L_a + 0.10 L_a sin(3.1415t)$	H
$\breve{\tau}_L$	0	Nm

DE variants in the tracking control problem, the DC motor is persistently excited by an input over both, the bandwidth and the full amplitude range of the system, however with the regulation control problem this does not happen. Hence, with out a persistently excited input, the convergence of the algorithm tends to local minimum which implies an increase in the velocity error. It is important to remark that the mean runtime by DEC2B-DF and DEB1B-EP was around $0.3171s$.

Non-parametric statistical tests were applied to the results obtained in the samples of runs in Table 6. As a first step, the 95%-confidence Kruskal-Wallis and 95%-confidence Friedman tests were applied. Table 7 summarizes the p-values obtained. According to those results, in the four control problems (RCP-TVP1, RCP-TVP2, TCP-TVP1,TCP-TVP2) significance differences among the four DE variants were reported. To get a closer look into the statistical significance of results, the 95%-confidence Wilcoxon test was applied to pair-wise comparisons between DE variants per each problem instance. The obtained p-values are reported in Table 8, where

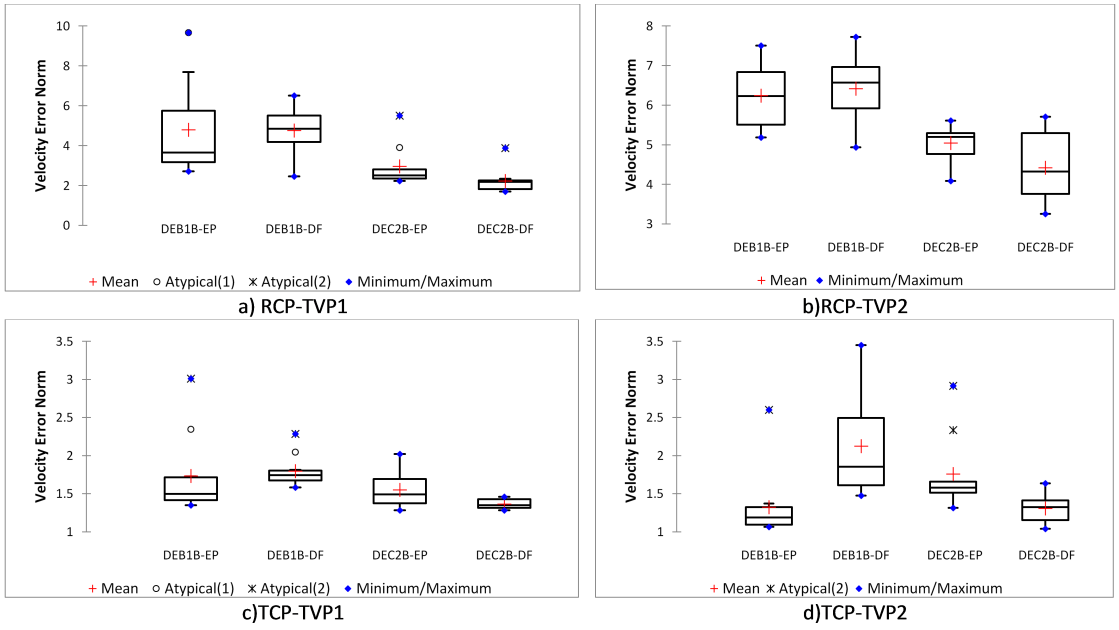

Figure 2: Box plots of the results obtained by the four DE-variants.

most of the results provided by the Kruskal-Wallis and Friedman tests were confirmed, and the significance improvement with a level of significance $\alpha = 0.5$ is shown in bold face. The exceptions were mainly attributed in the case DEB1B-EP / DEB1B-DF, where no significant differences in three problems (RCP-TVP1, RCP-TVP2, and TCP-TVP1) were found. The other cases with no significant differences were DEC2B-EP / DEB1B-EP in test problems TCP-TVP1 and TCP-TVP2; DEC2B-DF / DEB1B-EP in problem TCP-TVP2; and finally DEC2B-EP / DEB1B-DF in the same test problem TCP-TVP2. The boxplots generated by the statistical results are presented in Figure 2.

From the results showed in Tables 6, 7, 8, and Figure 2, the following findings are remarked: DEC2B-DF outperformed the other three variants in three problems: RCP-TVP1, RCP-TVP2, and TCP-TVP1. Regarding the remaining test

problem TCP-TVP2, DEC2B-DF provided the best performance among DEC2B-EP and DEB1B-DF. Nevertheless, the DEC2B-DF and DEB1B-EP presents a similar behavior in the test problem TCP-TVP2. Through the previous analysis, it can be concluded that the set of feasibility rules combined with the arithmetic crossover promoted by the DE/current-to-best/1 variant, were the most suitable for the proposed DE-based adaptive control when dealing with the four problem instances tackled in this work.

Table 6: Results obtained by each DE variant in each one of the four problem instances. Results with trajectory velocity error more than 5% with respect to the desired velocity trajectory (unacceptable results) are marked with "-". Best statitical results are marked with boldface.

Run	$\|\dot{\mathbf{e}}(\mathbf{t})\|$ rad/s $\forall$ t $\in [1.6, 6]$s by each DE variant			
	DEB1B-EP	DEB1B-DF	DEC2B-EP	DEC2B-DF
1	2.9641	3.4142	2.5048	1.9645
2	5.8824	4.8499	2.3579	3.8882
3	3.4199	-	2.3067	1.6994
4	3.8861	5.3991	5.5118	2.1799
5	2.7179	4.679	2.2367	1.7826
6	9.6626	6.5084	2.7207	2.2266
7	7.6951	5.5136	3.908	1.7732
8	3.3285	5.8719	-	2.3436
9	5.3663	2.465	2.8082	2.2602
10	3.1186	4.189	2.372	2.2001
Mean	4.8042	4.7656	2.9696	**2.2318**
Median	3.653	4.8499	2.5048	**2.19**
S. D.	2.3323	1.2594	1.0814	**0.6261**

a) Control Problem: RCP-TVP1

Run	$\|\dot{\mathbf{e}}(\mathbf{t})\|$ rad/s $\forall$ t $\in [1.6, 6]$s by each DE variant			
	DEB1B-EP	DEB1B-DF	DEC2B-EP	DEC2B-DF
1	6.9538	6.5687	-	5.4969
2	7.5022	6.9558	5.2931	3.2533
3	-	7.7221	5.6116	4.3257
4	-	5.5069	4.6116	4.4052
5	-	-	5.2807	5.2921
6	5.9647	4.9392	4.766	5.7081
7	5.3584	6.9657	4.0889	3.6742
8	-	7.052	5.0047	-
9	5.0047	6.1263	5.5646	3.7599
10	6.4904	5.923	5.1967	3.8898
Mean	6.2425	6.4177	5.0464	**4.4228**
Median	6.2276	6.5687	5.1967	**4.3257**
S. D.	0.9089	0.8705	**0.4890**	0.8820

b) Control Problem: RCP-TVP2

Run	$\|\dot{\mathbf{e}}(\mathbf{t})\|$ rad/s $\forall$ t $\in [1.6, 6]$s by each DE variant			
	DEB1B-EP	DEB1B-DF	DEC2B-EP	DEC2B-DF
1	3.0121	2.2859	1.3993	1.3228
2	1.4333	1.7801	1.7366	1.311
3	1.3505	1.7481	1.7098	1.4452
4	1.3885	1.7162	1.6466	1.4091
5	1.6834	2.045	1.5854	1.4356
6	1.7265	1.5811	1.2843	1.3564
7	1.4952	1.7379	1.3611	1.3405
8	1.4968	1.8127	1.3826	1.4601
9	2.3463	1.6597	1.3728	1.2841
10	1.4089	1.6173	2.0222	1.2971
Mean	1.73415	1.7984	1.55007	**1.36619**
Median	1.496	1.743	1.49235	**1.34845**
S. D.	0.5361	0.2138	0.2315	**0.0658**

c) Control Problem: TCP-TVP1

Run	$\|\dot{\mathbf{e}}(\mathbf{t})\|$ rad/s $\forall$ t $\in [1.6, 6]$s by each DE variant			
	DEB1B-EP	DEB1B-DF	DEC2B-EP	DEC2B-DF
1	1.1658	1.829	1.5768	1.4196
2	1.2108	2.6438	1.6599	1.1213
3	2.6003	1.4769	1.6541	1.3897
4	1.3707	1.8798	1.584	1.4605
5	1.0995	2.0412	2.3379	1.3515
6	1.2115	1.5632	2.918	1.1315
7	1.09	3.0749	1.3157	1.0414
8	1.0643	1.7569	1.5017	1.6356
9	1.0748	3.4493	1.5433	1.2986
10	1.3602	1.5431	1.4875	1.2216
Mean	1.3248	2.1258	1.7579	**1.3071**
Median	**1.1883**	1.8544	1.5804	1.3251
S. D.	0.4616	0.6904	0.4883	**0.1814**

d) Control Problem: TCP-TVP2

Table 7: Results of the 95%-confidence Kruskal-Wallis and Friedman tests.

Problem instance	p-value	
	Kruskall-Wallis test	**Friedman test**
RCP-TVP1	<0.0001	0.0013
RCP-TVP2	0.001	0.0406
TCP-TVP1	0.001	0.0018
TCP-TVP2	<0.0001	0.0004

Table 8: Results of the 95%-confidence Wilcoxon signed-rank test.

DE variants	p-value			
	RCP-TVP1	**RCP-TVP2**	**TCP-TVP1**	**TCP-TVP2**
DEC2B-DF versus DEC2B-EP	**0.038**	**0.04**	**0.016**	**0.005**
DEC2B-DF versus DEB1B-EP	**0.003**	**0.018**	**0.01**	0.762
DEC2B-DF versus DEB1B-DF	**0.005**	**0.01**	**0.003**	**0.003**
DEC2B-EP versus DEB1B-EP	**0.022**	**0.053**	0.342	0.979
DEC2B-EP versus DEB1B-DF	**0.021**	**0.007**	**0.021**	0.131
DEB1B-EP versus DEB1B-DF	0.639	0.583	0.238	**0.021**

5.2. Comparison against a traditional control technique

After identifying the most competitive DE variant, its performance was compared against the Proportional-Integral control (PIC). DEC2B-DF is identified as Differential Evolution Based Adaptive Control (DEBAC) in this simulation test. The proportional gains and the integral ones of the PIC are chosen as $\bar{k}_p = 0.15$ and $\bar{k}_i = 12.9904$, respectively. Those proposed gains were obtained through a rigours trial and error procedure where the used values in the paper are those that provide the best performance function among trials.

In Table 9, the comparison of the control systems performance was made by computing the three commonly used control performance indexes [20]: the Integral Absolute Error (IAE) given by $\int_1^6 |e(t)|\, dt$, the Integral Time-weighted Absolute Error

(ITAE) represented by $\int_1^6 t \cdot |e(t)|\, dt$ and the Integral Squared Error (ISE) given by $\int_1^6 e^2 dt$.

The results obtained by both approaches show that DEBAC clearly outperformed PIC in the four problem instances based on the three error measures (see mean and median values in Table 9). With those results, the findings are stated as follows for the Regulation Control Problem (RCP) and the Trajectory Control Problem (TCP): *i*) the DEBAC improvements for the IAE with respect to PIC were around 83.32% and 99.34%, respectively. Such values suggest that DEBAC efficiently reduced the velocity error oscillation induced by time varied parameters of the DC motor; *ii*) the DEBAC improvements for the ITAE with respect to PIC were around 83.31% and 99.27%, respectively. With the ITAE index, the analysis was focused on the velocity error after the settling time. Hence, DEBAC presented smaller error in the stabilization and tracking of the velocity of the DC motor. Finally, *iii*) the DEBAC improvements for the ISE with respect to PIC were around 92.49% and 99.99%, respectively. Such behavior indicates that DEBAC provided a low amplitude velocity error band.

Table 9: Comparative results of the performance criteria for the DEBAC and PIC approaches.

RCP-TVP1			
	IAE	ITAE	ISE
MEAN	191.7617	584.7208	111.1628
MEDIAN	191.7617	584.7208	111.1628
S.D.	**0**	**0**	**0**

a) **PIC**

RCP-TVP1			
	IAE	ITAE	ISE
MEAN	**34.2405**	**102.234**	**8.3504**
MEDIAN	**31.9373**	**95.6884**	**5.646**
S.D.	6.0609	20.0381	5.6044

b) **DEBAC**

RCP-TVP2			
	IAE	ITAE	ISE
MEAN	484.0223	1683.209	288.7147
MEDIAN	484.0223	1683.209	288.7147
S.D.	**0**	**0**	**0**

c) **PIC**

RCP-TVP2			
	IAE	ITAE	ISE
MEAN	**82.6115**	**281.7535**	**19.9969**
MEDIAN	**81.1991**	**281.0921**	**15.6258**
S.D.	6.9297	18.5411	11.999

d) **DEBAC**

TCP-TVP1			
	IAE	ITAE	ISE
MEAN	5176.836	18006.33	33078.68
MEDIAN	5176.836	18006.33	33078.68
S.D.	**0**	**0**	**0**

e) **PIC**

TCP-TVP1			
	IAE	ITAE	ISE
MEAN	**35.4370**	**122.2728**	**2.7226**
MEDIAN	**34.3451**	**117.4929**	**2.1015**
S.D.	3.1482	12.1586	1.3390

f) **DEBAC**

TCP-TVP2			
	IAE	ITAE	ISE
MEAN	5161.922	17909.65	33074.92
MEDIAN	5161.922	17909.65	33074.92
S.D.	**0**	**0**	**0**

g) **PIC**

TCP-TVP2			
	IAE	ITAE	ISE
MEAN	**36.61931**	**131.2836**	**4.72944**
MEDIAN	**36.24145**	**125.8612**	**2.1403**
S.D.	7.105131	20.02316	8.385448

h) **DEBAC**

To provide further evidence on the different performances provided by DEBAC and PIC, in Figs. 3-6 the simulation results of the velocity, voltage and current signal behavior in both control problems (RCP-TVP and TCP-TVP) using DEBAC (Figs. 3-6b and Figs. 3-6d), and PIC (Figs. 3-6a and Figs. 3-6c) are shown. The dotted line represents the desired velocity w_r, while the continuous line is the current

angular velocity of the motor x_2. Only in the regulation control problem (RCP), the time-variant parameters impact on the stabilization of the DC motor (see the time when the uncertainties are presented in Fig. 3a-b and Fig. 4a-b). This behavior looks like noise in the control signal (input voltage) and is attributed to the kind of control problem (regulation control problem) and the uncertainties presented in the DC motor dynamics. Without uncertainties (for $t \in [0, 2] \bigcup [4, 6]$ in Fig. 3) the noise disappears in the control signal of DEBAC but when the uncertainties are applied (for $t \in [2, 4]$) the noise appears. This behavior is attributed to the lack of the reference signal periodicity in the regulation control problem which results in a more complex problem with a multi-modal behavior when the uncertainties appear in the DC motor dynamic. Such lack of reference signal periodicity reduce at minimum the excitation of the DC motor frequencies making more difficult to obtain the control parameter $\bar{p}$. Therefore such noisy behavior in the control signals compensates as possible, the non-linear uncertainties. Based on the simulation results in Figs. 3-6 and on the analysis of Table 9, it can be concluded that DEBAC presents a better angular velocity, stabilization, and tracking of the DC motor towards the reference velocity than those provided by PIC, under the effect of time-variant parameters. In addition, based on the power consumption using for each controller (voltage and current applied the DC motor), the DEBAC presents a small increment of 3.5%, 7.7%, 2.7% and 3.2% for the RCP-TVP1, RCP-TVP2, TCP-TVP1 and TCP-TVP2, respectively with respect to the PIC. This energy consumption increment in the DEBAC corresponds to a better velocity regulation of the DC motor due to control signal requires more energy to efficiently compensate the uncertainties and therefore the amplitude in the control signal and its current by using DEBAC are larger than PIC. Finally, it was observed that in both control systems, the voltage signal (control signal) satisfied the control signal bounds.

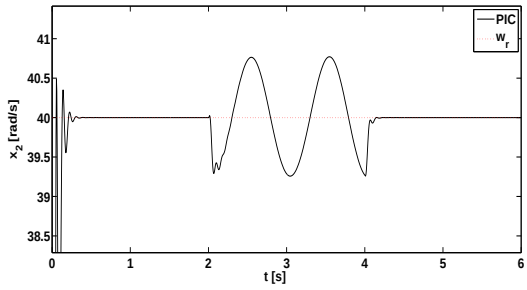

a) PIC: Motor's velocity (zoom)

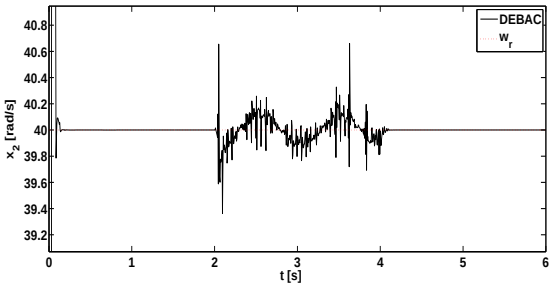

b) DEBAC: Motor's velocity (zoom)

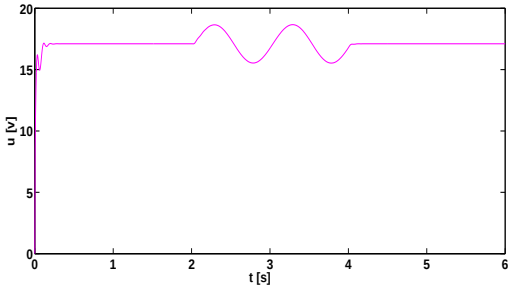

c) Control signal provided by PIC

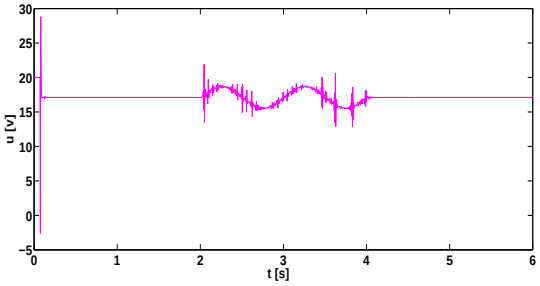

d) Control signal provided by DEBAC

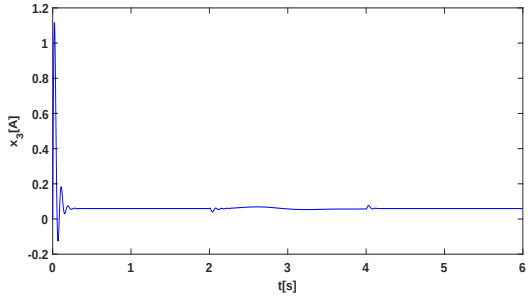

e) PIC: Motor's armature current

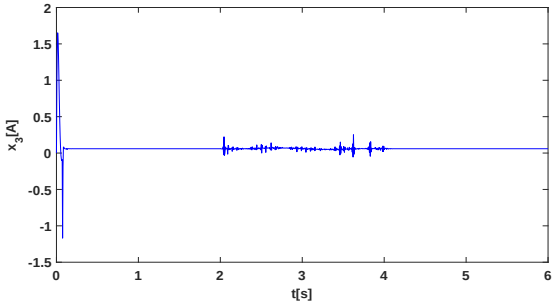

f) DEBAC: Motor's armature current

Figure 3: Behavior of the angular velocity, input voltage (control signal) and current of the DC motor for the PIC and the DEBAC in the RCP-TVP1.

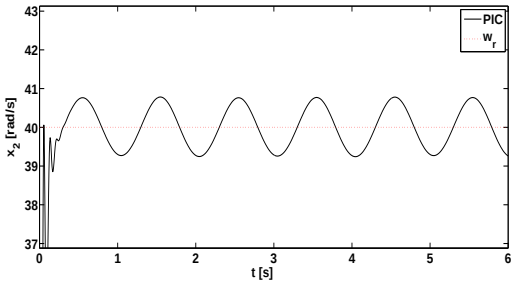

a) PIC: Motor's velocity (zoom)

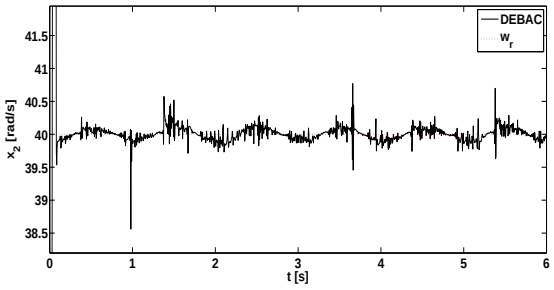

b) DEBAC: Motor's velocity (zoom)

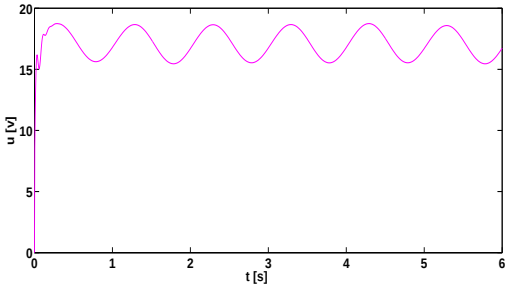

c) Control signal provided by PIC

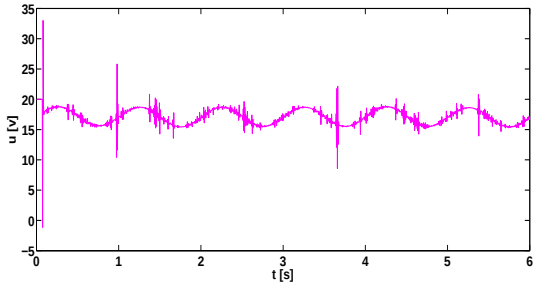

d) Control signal provided by DEBAC

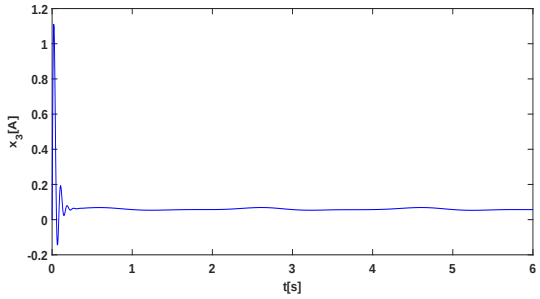

e) PIC: Motor's armature current

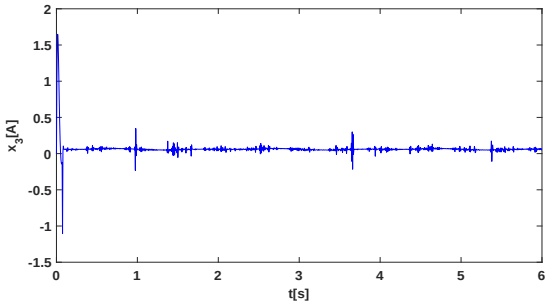

f) DEBAC: Motor's armature current

Figure 4: Behavior of the angular velocity, input voltage (control signal) and current of the DC motor for the PIC and DEBAC in the RCP-TVP2.

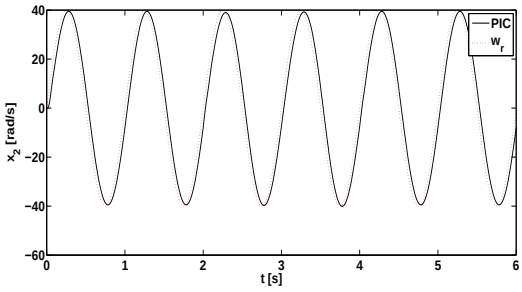

a) PIC: Motor's velocity (zoom)

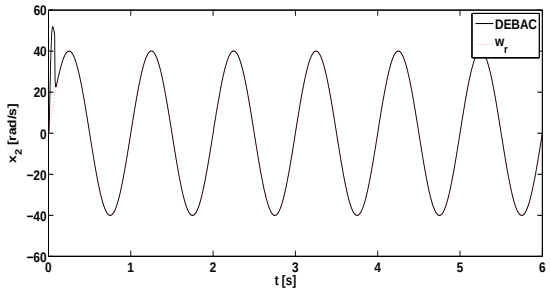

b) DEBAC: Motor's velocity (zoom)

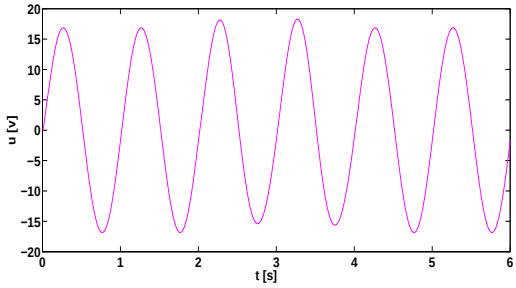

c) Control signal provided by PIC

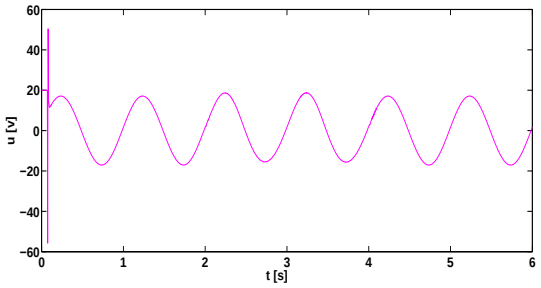

d) Control signal provided by DEBAC

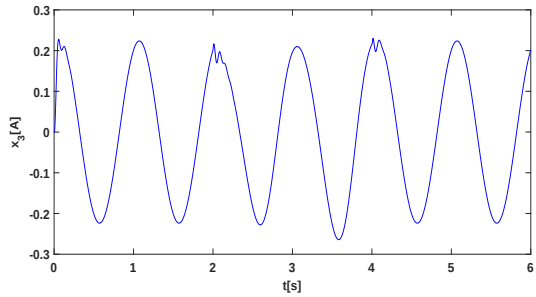

e) PIC: Motor's armature current

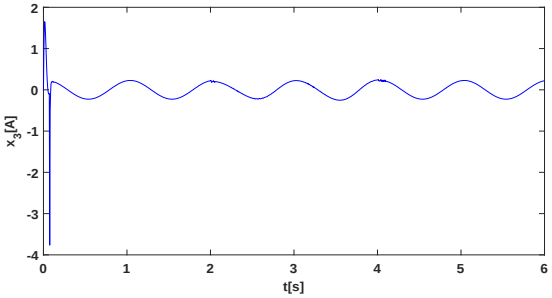

f) DEBAC: Motor's armature current

Figure 5: Behavior of the angular velocity, input voltage (control signal) and current of the DC motor for the PIC and DEBAC in the TCP-TVP1.

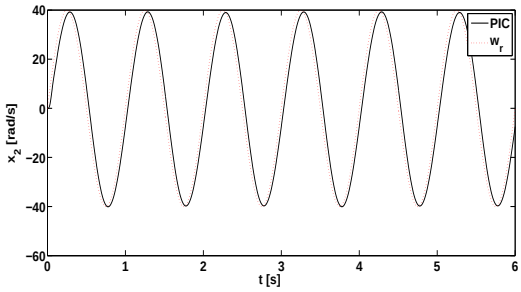

a) PIC: Motor's velocity (zoom)

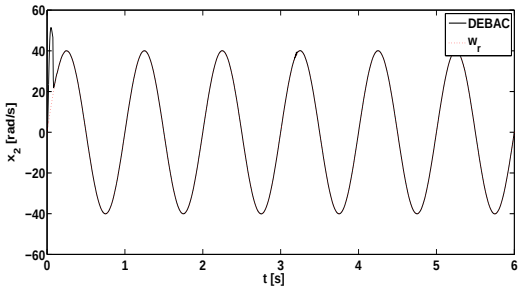

b) DEBAC: Motor's velocity (zoom)

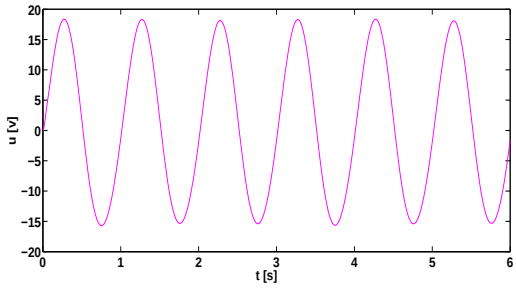

c) Control signal provided by PIC

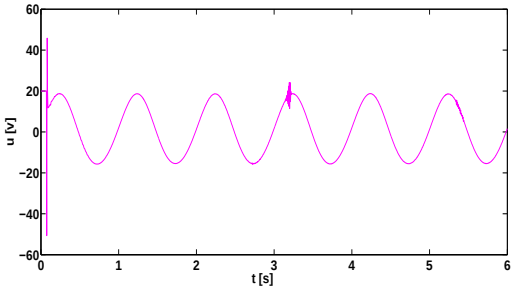

d) Control signal provided by DEBAC

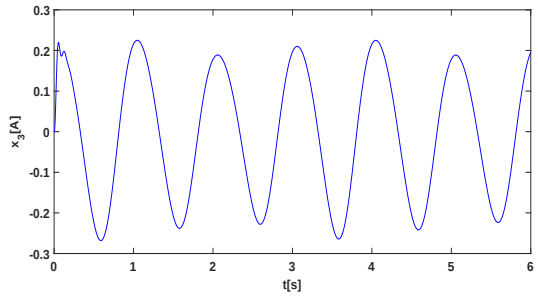

e) PIC: Motor's armature current

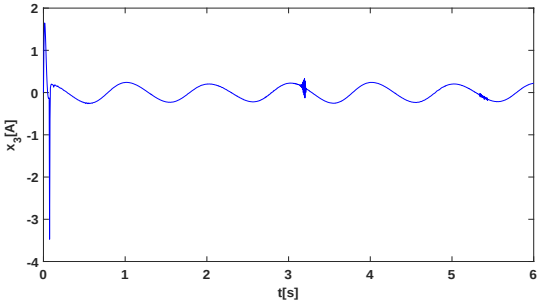

f) DEBAC: Motor's armature current

Figure 6: Behavior of the angular velocity, input voltage (control signal) and current of the DC motor for the PIC and DEBAC in the TCP-TVP2.

On the other hand, in order to show the behavior of the DEBAC with a nonlinear load, a pendulum system is incorporated into the shaft of the DC motor. Such dynamics modifies the inertia and the load torque of the DC motor parameters as

follows: $\breve{J}_0 = J_0 + (I + ml_c^2)$ and $\breve{\tau}_L = (ml_c g sin(x_1))$ where the pendulum parameters are the mass $m = 0.1604kg$, the mass center length $l_c = 0.06032m$ and the inertia $I = 6.5465E - 4kgm^2$, respectively, and the term $g = 9.81m/s^2$ is the gravitational acceleration. The rest of the DC motor parameters are set according to their nominal ones. In Fig. 7 and 8, the behavior of the PIC and DEBAC with the pendulum as load is displayed for the velocity regulation and the velocity tracking. It is observed that the DEBAC outperforms the performance of the PIC such that the velocity error is decreased. With reference to the energy consumption a similar behavior is presented as in the previous cases (RCP-TVP1, RCP-TVP2, TCP-TVP1, TCP-TVP2), i.e., a small increment of the energy consumption is presented in the DEBAC because of a better compensation of the nonlinear load. This indicates that the proposal DEBAC efficiently compensates the nonlinear behavior due to a robotic manipulator dynamics, and hence the proposal may be used in the control of complex system.

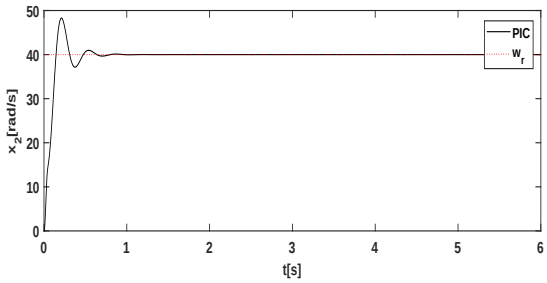

a) PIC: Motor's velocity (zoom)

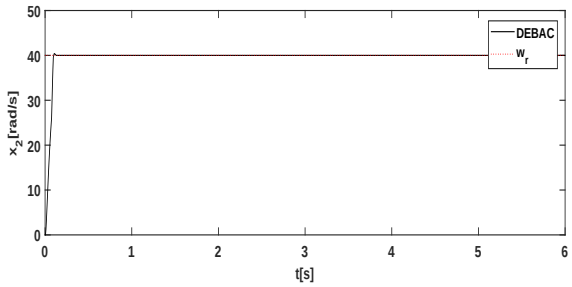

b) DEBAC: Motor's velocity (zoom)

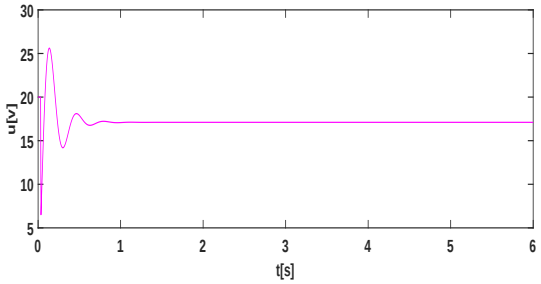

c) Control signal provided by PIC

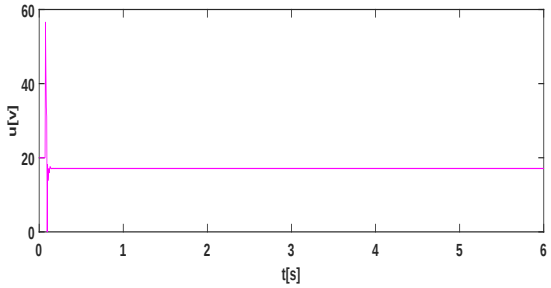

d) Control signal provided by DEBAC

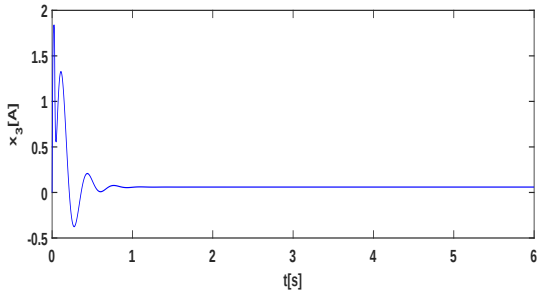

e) PIC: Motor's armature current

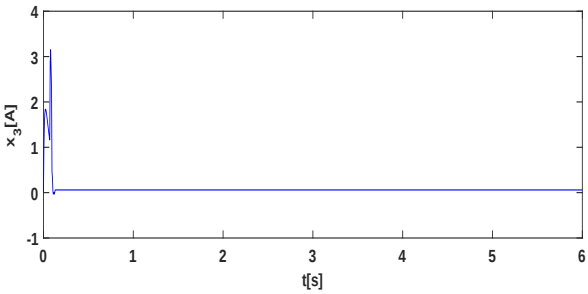

f) DEBAC: Motor's armature current

Figure 7: Behavior of the angular velocity, input voltage (control signal) and current of the DC motor for the PIC and DEBAC with a pendulum as load in the regulation problem.

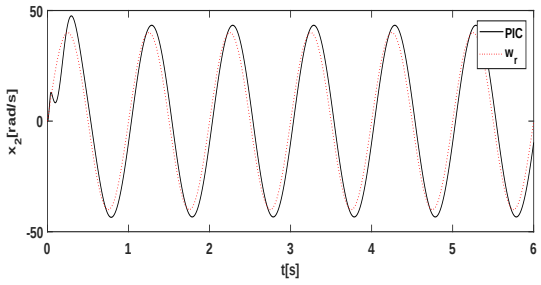

a) PIC: Motor's velocity (zoom)

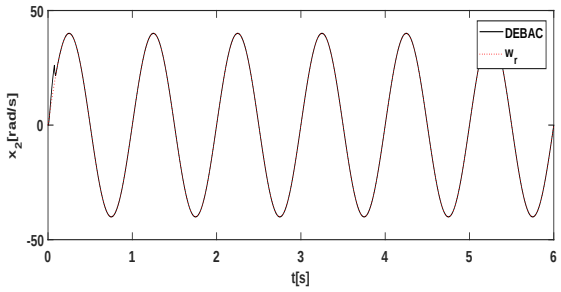

b) DEBAC: Motor's velocity (zoom)

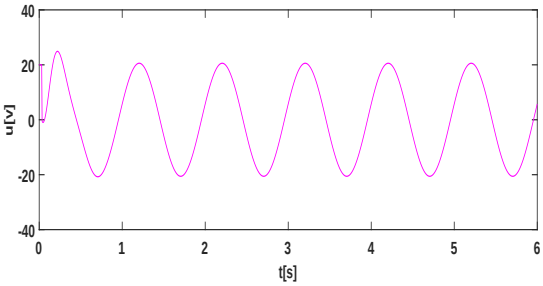

c) Control signal provided by PIC

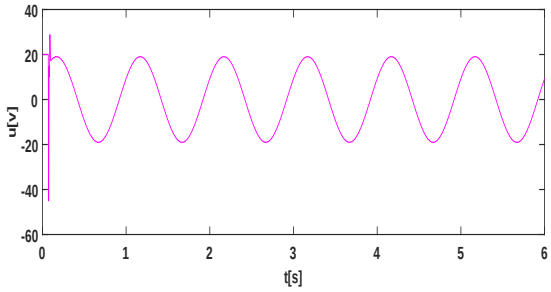

d) Control signal provided by DEBAC

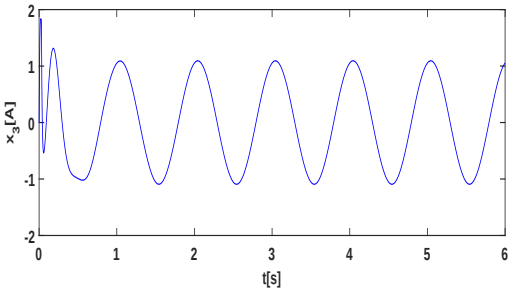

e) PIC: Motor's armature current

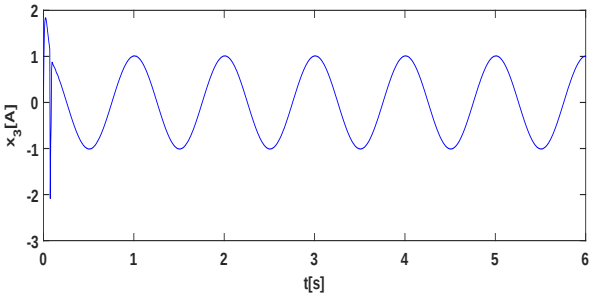

f) DEBAC: Motor's armature current

Figure 8: Behavior of the angular velocity, input voltage (control signal) and current of the DC motor for the PIC and DEBAC with a pendulum as load in the tracking problem.

6. Conclusions

In this paper, an alternative control of a DC motor based on a differential evolution (DE) adaptation was proposed. The dynamic optimization problem for the

differential evolution based control adaptation (DEBAC) was stated. The design of the search algorithm was obtained by an empirical study of two DE variants combined with two different constraint-handling techniques (an exterior penalty function and a set of feasibility rules). The main highlights of such empirical comparison were the following:

- In the regulation control problem, the more reliable DE variant was DEC2B-DF because only one unacceptable result was provided. In the tracking control problem, all studied variants were reliable.

- The most competitive DE variant was DEC2B-DF. Hence, the constraint-handling technique based on the feasibilty rules coupled with the arithmetic crossover of DE/current-to-best/1 promoted a more suitable search and hence the importance of analysing the contraint handling in the control tuning using EAs.

The so-called DEBAC (DEC2B-DF from the empirical comparison abovementioned) efficiently handled with time-variant parameters in the DC motor with acceptable closed loop systems performance. The results provided by DEBAC showed a superior performance in the stabilization and tracking of the motor's velocity when compared against a Proportional-Integral control (PIC). From that comparison between DEBAC and PIC the findings were the following:

- DEBAC reduced the velocity error oscillation and the amplitude velocity error band due to time varied parameters of the DC motor. Therefore, DEBAC presented better angular velocity stabilization and tracking values of the DC motor than those obtained by PIC.

- The angular velocity error provided by DEBAC was reduced around 83% compared with the error obtained by PIC.

The future work will cover the analysis of DE variants in parallel computing paradigm for the laboratory testing purposes (real time implementation), the solution of the problem as a multi-objective optimization problem by using evolutionary algorithms and the performance analysis of the DEBAC in complex systems.

Acknowledgements

The first author acknowledges support from the Secretaría de Investigación y Posgrado del Instituto Politécnico Nacional (SIP-IPN) under project number $SIP-20170783$, $SIP-20172317$ and CONACYT under project number 281728. The second author acknowledges suport from CONACyT through project No. 220522. The third author acknowledges support from CONACYT through a scholarship to pursue graduate studies at the National Laboratory of Advanced Informatics.

References

[1] S. Algoul, M. Alam, M. Hossain, M. Majumder, Multi-objective optimal chemotherapy control model for cancer treatment, Méd. and Biol. Eng. and Comput. 49 (2011) 51–65.

[2] K. J. Astrom, B. Wittenmark, Adaptive Control, Prentice Hall, 1994.

[3] M. S. Bazaraa, H. D. Sherali, C. M. Shetty, Nonlinear Programming: Theory and Algorithms, Wiley-Interscience, 2006.

[4] B. Bhushan, M. Bhushan, Adaptive control of DC motor using bacterial foraging algorithm, Appl. Soft Comput. 11 (8) (2011) 4913–4920.

[5] J. Chiasson, Modeling and High Performance Control of Electric Machines, Wiley-IEEE Press, 2005.

[6] S. Das, P. N. Suganthan, Differential evolution: a survey of the state-of-the-art, IEEE Trans. On Evol. Comput. 15 (1) (2011) 4–31.

[7] K. Deb, An efficient constraint handling method for genetic algorithms, in: Computer Methods in Applied Mechanics and Engineering, 311–338, 1998.

[8] A. E. Eiben, J. E. Smith, Introduction to Evolutionary Computing, Natural Computing Series, Springer Verlag, 2003.

[9] P. Fleming, R. Purshouse, Evolutionary algorithms in control systems engineering: a survey, Control Eng. Practice 10 (11) (2002) 1223 – 1241.

[10] A. Herreros, E. Baeyens, J. R. Perán, Design of PID-type controllers using multiobjective genetic algorithms, {ISA} Trans. 41 (4) (2002) 457 – 472.

[11] A. Isidori, Nonlinear Control Systems, Springer-Verlag Berlin and Heidelberg GmbH & Co. K., 1995.

[12] R. Krishnan, Electric Motor Drives: Modeling, Analysis and Control, Prentice Hall, 2001.

[13] E. V. Kumar, G. S. Raaja, J. Jerome, Adaptive PSO for optimal LQR tracking control of 2 DoF laboratory helicopter, Appl. Soft Comput. 41 (2016) 77 – 90.

[14] M. López-Ibánez, J. Dubois-Lacoste, T. Stützle, M. Birattari, The irace package, iterated race for automatic algorithm configuration, Tech. Rep. TR/IRIDIA/2011-004, IRIDIA, Université Libre de Bruxelles, Belgium, URL `http://iridia.ulb.ac.be/IridiaTrSeries/IridiaTr2011-004.pdf`, 2011.

[15] S. E. Lyshevski, Nonlinear control of mechatronic system with permanent-magnet DC motors, Mechatron. 9 (5) (1999) 539–552.

[16] E. Mezura-Montes, C. A. Coello-Coello, Constraint-handling in nature-inspired numerical optimization: past, present and future, Swarm and Evol. Comput. 1 (4) (2011) 173–194.

[17] E. Mezura-Montes, M. E. Miranda-Varela, R. Gómez-Ramón, Differential evolution in constrained numerical optimization. An empirical study, Inf. Sci. 180 (22) (2010) 4223–4262.

[18] E. Mezura-Montes, J. Velázquez-Reyes, C. A. Coello-Coello, Comparing differential evolution models for global optimization, in: 2006 Genetic and Evolutionary Computation Conference (GECCO'2006), vol. 1, 485–492, 2006.

[19] R. Morale, H. S.-R. J.A. Somolinos, Control of a DC motor using algebraic derivative estimation with real time experiments, Measurements 47 (2014) 401–417.

[20] K. Ogata, Modern Control Engineering, Prentice Hall, 2009.

[21] R. Orteg, M. W. Spong, Adaptive motion control of rigid robots: a tutorial, Automatica 25 (1989) 877–888.

[22] K. Price, R. M. Storn, J. A. Lampinen, Differential Evolution: A Practical Approach to Global Optimization, Springer, 2005.

[23] G. Reynoso-Meza, X. Blasco, J. Sanchis, M. Martínez, Controller tuning using evolutionary multi-objective optimisation: current trends and applications, Control Eng. Practice 28 (2014) 58 – 73.

[24] J. Romero-Pérez, O. Arrieta, F. Padula, G. Reynoso-Meza, S. Garcia-Nieto, P. Balaguer, Estudio comparativo de algoritmos de auto-ajuste de controladores PID. Resultados del benchmark 2010-2011 del grupo de ingeniería de control de {CEA}, Rev. Iberoam. de Autom. e Inform. Industrial {RIAI} 9 (2) (2012) 182 – 193.

[25] P. Siarry, Z. Michalewicz (Eds.), Advances in Metaheuristic Methods for Hard Optimization, Springer, Berlin, 2008.

[26] M. W. Spong, S. Hutchinson, M. Vidyasagar, Robot Modeling and Control, John Wiley & Sons, inc., 2005.

[27] C. Thang, P. Miller, V. Krovy, J.-C. Ryu, S. Agrawal, Differential flatness-based planning and control of a wheeled mobile manipulator theory and experiment, IEEE/ASME Trans. on Mechatron. 16 (4) (2011) 768–773, ISSN 1083-4435.

[28] F. Wang, X. Zhao, D. Zhang, Z. Ma, X. Jing, Robust and precision control for a directly-driven XY table, Proceedings of the Institution of Mechanical Engineers, Part C: Journal of Mechanical Engineering Science 225 (5) (2011) 1107–1120.

[29] N. Öztürk, E. Çelik, Speed control of permanent magnet synchronous motors using fuzzy controller based on genetic algorithms, Int. J. of Electr. Power & Energy Syst. 43 (1) (2012) 889 – 898.

List of figure captions:

Figure 1: Schematic diagram of the dynamic optimization process for the on-line control parameter estimation.

Figure 2: Box plots of the results obtained by the four DE-variants.

Figure 3: Behavior of the angular velocity, input voltage (control signal) and current of the DC motor for the PIC and the DEBAC in the RCP-TVP1.

Figure 4: Behavior of the angular velocity, input voltage (control signal) and current of the DC motor for the PIC and the DEBAC in the RCP-TVP2.

Figure 5: Behavior of the angular velocity, input voltage (control signal) and current of the DC motor for the PIC and the DEBAC in the TCP-TVP1.

Figure 6: Behavior of the angular velocity, input voltage (control signal) and current of the DC motor for the PIC and the DEBAC in the TCP-TVP2.

Figure 7: Behavior of the angular velocity, input voltage (control signal) and current of the DC motor for the PIC and DEBAC with a pendulum as load in the regulation problem.

Figure 8: Behavior of the angular velocity, input voltage (control signal) and current of the DC motor for the PIC and DEBAC with a pendulum as load in the tracking problem.

List of table captions:

Table 1: Parameters of the DE variants by using the iRace package.

Table 2: Limits of the design variable vector $\bar{p}$.

Table 3: Nominal parameters (NomP) of the DC Motor.

Table 4: Parameter TVP1: Time-variant parameters (TVP) of the DC motor. Those can be grouped in $\breve{p} \in R^6$.

Table 5: Parameter TVP2: Time-variant parameters (TVP) of the DC motor. Those can be grouped in $\breve{p} \in R^6$.

Table 6: Results obtained by each DE variant in each one of the four problem instances. Results with trajectory velocity error more than 5% with respect to the desired velocity trajectory (unacceptable results) are marked with "-". Best statitical results are marked with boldface.

Table 7: Results of the 95%-confidence Kruskal-Wallis and Friedman tests.

Table 8: Results of the 95%-confidence Wilcoxon signed-rank test.

Table 9: Comparative results of the performance criteria for the DEBAC and PIC approaches.